

Article

Cooling Performance Enhancement of a 20 RT (70 kW) Two-Evaporator Heat Pump with a Vapor–Liquid Separator

Won-Suk Yang¹ and Young Il Kim^{2,*}

¹ Department of Architectural Engineering, Graduate School, Seoul National University of Science and Technology, Seoul 01811, Korea; wsyang1004@nate.com
² School of Architecture, Seoul National University of Science and Technology, Seoul 01811, Korea
* Correspondence: yikim@seoultech.ac.kr; Tel.: +82-2-970-6557

Abstract: 20 RT (70 kW) two-evaporator heat pump system was developed, manufactured, and tested to enhance the cooling performance using a vapor–liquid separator. In the proposed system, two evaporators are connected in series, and the refrigerant passing through the primary evaporator is separated into vapor and liquid using a vapor–liquid separator. The vapor refrigerant is passed to the compressor, whereas the liquid phase flows into the second evaporator. The amount of vapor refrigerant sent to the compressor can be adjusted through a needle valve opening (0%, 50%, and 100%). The influence of this parameter on the cooling performance was analyzed. The cooling performance tests were repeated five times to check repeatability. Data associated with the air and refrigerant sides were obtained, and the average coefficients of performance (COPs) were calculated. The average COP associated with the air side was approximately 5% lower than that pertaining to the refrigerant side owing to the heat loss. In terms of the air-side cooling performance, the average COP was 3.14, 3.40, and 3.68 when the valve openings were 0%, 50%, and 100%, respectively. The cooling performance when the valve opening was 100% was 17.2% higher than that for the valve opening of 0%. The findings demonstrated that the cooling performance of a heat pump can be enhanced using two evaporators and a vapor–liquid separator.

Keywords: COP; heat pump; cooling; two-evaporator; refrigerant; vapor–liquid separator



Citation: Yang, W.-S.; Kim, Y.I. Cooling Performance Enhancement of a 20 RT (70 kW) Two-Evaporator Heat Pump with a Vapor–Liquid Separator. *Energies* **2022**, *15*, 3849. <https://doi.org/10.3390/en15113849>

Academic Editors: Sławomir Rabczak, Daniel Słysz and Krzysztof Nowak

Received: 4 April 2022
Accepted: 15 May 2022
Published: 24 May 2022

Publisher's Note: MDPI stays neutral with regard to jurisdictional claims in published maps and institutional affiliations.



Copyright: © 2022 by the authors. Licensee MDPI, Basel, Switzerland. This article is an open access article distributed under the terms and conditions of the Creative Commons Attribution (CC BY) license (<https://creativecommons.org/licenses/by/4.0/>).

1. Introduction

1.1. Background

Energy used for air conditioning in buildings is increasing to satisfy the improved quality of life and thermal comfort [1,2]. Moreover, the energy consumption of heating and cooling systems in buildings is rapidly increasing owing to the enhanced ventilation required to reduce COVID-19 infection through the air. The energy consumption of residential and commercial buildings in developed countries is 20–40% of the total, and the International Energy Agency (IEA) pointed out that the energy consumption of buildings accounts for 30–40% of the final energy consumption [3]. As shown in Figure 1, domestic building energy consumption corresponds to approximately 24% of the national energy consumption. Notably, the energy consumed by heating and cooling systems accounts for most (48.9%) of the total energy consumption in buildings [1].

Heat pump systems with high energy efficiency are widely used for the heating and cooling of buildings [3]. Heat pumps, as highly efficient devices, can perform both heating and cooling and supply more heat energy with less energy consumption [4,5]. Heat pump systems with high energy efficiency are widely used for the heating and cooling of buildings. Despite the use of a heat pump system, the amount of energy used for heating and cooling in buildings continues to increase. In particular, as the number of cooling systems increases due to climate change, energy consumption continues to increase [6]. Therefore, it was judged that it was necessary to study the improvement of the heat pump system to increase the cooling performance and save energy.

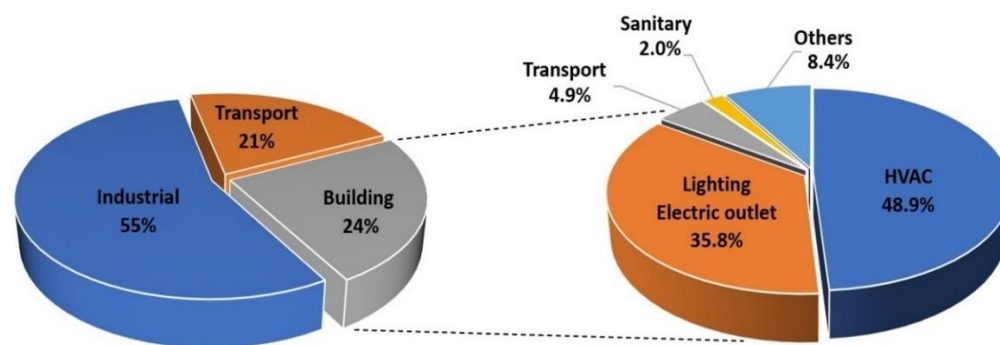


Figure 1. The type of energy consumption in buildings.

The cooling system of a heat pump cools the air as the liquid refrigerant flowing through the evaporator absorbs the surrounding thermal energy and evaporates. In general, all refrigerants do not evaporate and pass through the evaporator in a mixed state involving vapor and liquid forms. If the refrigerant drawn into the evaporator does not evaporate sufficiently, the capacity that the liquid accumulator can handle may be exceeded. In this case, the excess liquid refrigerant may flow into the compressor resulting in damage to the compressor [7]. Therefore, it was determined that cooling performance could be improved by configuring the two evaporators in series and evaporating the surplus liquid refrigerant that did not evaporate in the primary evaporator in the secondary evaporator. In addition, it was expected that it would be possible to achieve stable cooling when passing through the secondary evaporator by significantly cooling the air coming in from the primary evaporator. Wang et al. theoretically compared the thermodynamic performance of a two-stage evaporation vapor compression refrigeration cycle using refrigerants R290 (propane) and R600 (butane) with low global warming potential (GWP) and no ozone depletion potential (ODP) [8]. They showed that the COP of R600 was better than that of R134a, but their work was not based on an experiment. Yataganbaba et al. carried out an exergy analysis of R1234yf and R1234ze as R134a replacements in a two-evaporator vapor compression refrigeration system [9]. Their work proved that exergy analysis was a useful way of determining thermodynamic losses and optimizing the environmental and economic performance of a two-evaporator vapor compression refrigeration system, but the analysis was done with theoretical thermodynamic analysis and not actual measurements. In this work, however, the air-source two-evaporator vapor compression heat pump of cooling capacity 20RT (70 kW) was manufactured and tested in multi-environmental thermal chambers to obtain in situ measurement data. A theoretical study is good for qualitative analysis but cannot surpass the quantitative measurement obtained by experiment, which was adopted in this study. Although this vapor separation technology in the primary evaporator was applied and used in a water-source centrifugal turbo refrigeration system of large capacity, few works appear in the literature that analyzed the performance of this technology. This study is worthwhile because there are few works where a two-evaporator system was applied to a medium-sized capacity of air-source vapor compression refrigeration systems and performance measurement was carried out in actual operating conditions.

In this study, when two evaporators were connected in series and the vapor refrigerant from the outlet of the primary evaporator was sent to the compressor, the effect on the cooling performance of the heat pump was confirmed through an experiment.

1.2. Literature Review

Considerable research to enhance the heat pump performance has been performed in various domains, with the relevant studies focused on system design and improvement [10–13], control [14,15], building operation optimization [16,17], energy efficiency analyses [18–20] and comparison [21,22], and economic analyses [23,24].

Lee [25] constructed a double evaporator system to enhance heat pump performance. The power required for the compressor operation was decreased by controlling the refriger-

ant state with one expansion valve, thereby decreasing the fuel consumption by 1.4–3.0% and cooling efficiency by approximately 6–10%. Zhang et al. [26] demonstrated that the use of two evaporators could decrease the energy waste and high-temperature steam heat could be used to configure a system with a heat of evaporation of 1985 kg/h and COP of 4.92, which could be used in the industry. Through simulation-based analyses, Baik et al. [27] demonstrated that at a supply temperature of 60 °C, the heating performance associated with two heat pumps connected in series was approximately 5% higher than that of two pumps connected in parallel.

Elliott and Rasmussen [28] proposed a predictive control-based controller model that could effectively control multiple evaporators. Moreover, the authors attempted to increase the efficiency by controlling the amount of refrigerant supplied to the compressor by adjusting the expansion valves at the evaporator outlet according to the degree of superheat. Mei and Xia [29] proposed the autonomous hierarchical distributed control strategy to achieve the efficient operation of a two-evaporator air-conditioning system, which decreased the energy consumption by 38% and costs by 48.5%.

To decrease the energy consumption of a heat pump, Chen et al. [30] used a cooling device (ESD: Energy-Saving Device) that sent condensed water to a compressor. According to experiments in various indoor and outdoor conditions, the energy efficiency could be increased by approximately 25.4%. Chaiyat [31] attempted to decrease the temperature of the air entering the evaporation coil by using a phase-change material (PCM) to enhance the cooling efficiency of the air conditioner. In an experiment involving a PCM of approximately 40 cm, the average daily power consumption of the air conditioner decreased by approximately 3.09 kWh, corresponding to annual cost savings of 170.03 USD.

1.3. Objectives and Limits of Research

In the literature review, it was possible to confirm the study of improving the energy performance through the improvement of the performance of the heat exchanger and the control of the heat pump. The vapor generated in the evaporator no longer contributes to cooling and acts as a resistance to the refrigerant flow. In this study, a heat pump consisting of two evaporators was conducted to reduce the power consumption of the compressor while improving the cooling performance of the evaporator by reducing the refrigerant flow resistance by sending the vapor generated from the evaporator to the compressor. If two evaporators are used, the heat exchanger area can be reduced compared to using one evaporator of the same capacity, resulting in a smaller product size. Furthermore, like a general heat pump system, a heating operation is possible by reversing the cooling cycle with a four-way valve. It is expected that this study will be used as basic data for a heat pump system that improves energy performance by reducing the flow resistance of refrigerants with multiple evaporators and, at the same time, reducing the power consumption of the compressor.

For the cooling performance test, standard climate evaluation conditions were applied in the national standard test conditions for air-cooled heat pumps (KS B ISO 13253). Under standard climate evaluation conditions, the outdoor dry-bulb temperature and the air conditioner inlet dry-bulb temperature are 35 °C and 27 °C, respectively [31]. Depending on the characteristics of the heat pump during cooling, if the outdoor temperature is higher than the experimental conditions, the condenser efficiency is lowered, hence the cooling performance is lowered; however, in the opposite case, the performance is higher. On the other hand, if the temperature entering the air conditioner is low, the evaporator efficiency is lowered, but in the opposite case, it is increased. Therefore, it was judged that the results of this study were significantly affected when the outdoor temperature was low or the air conditioner inlet temperature was high compared to the experimental conditions.

2. Materials and Methodology

In this study, a 20 RT (70 kW) air conditioner to which a two-evaporator heat pump system configured with two evaporators in series was applied was tested. RT (Refrigeration

Ton) is a unit for representing capacities of heat pumps or refrigeration devices and is equivalent to 3.517 kW. Thus, 20 RT is equivalent to about 70 kW. In the two-evaporator system, the refrigerant passing through the primary evaporator is separated into vapor and liquid refrigerants through a vapor–liquid separator. The vapor refrigerant is sent to the compressor and the liquid refrigerant is sent to the secondary evaporator. The effect of the amount of vapor refrigerant input to the compressor on the cooling performance of the heat pump was examined. The amount of vapor refrigerant was adjusted through the opening of a needle valve [32] (0%, 50%, and 100% in this study).

Figure 2 shows the research flow chart.

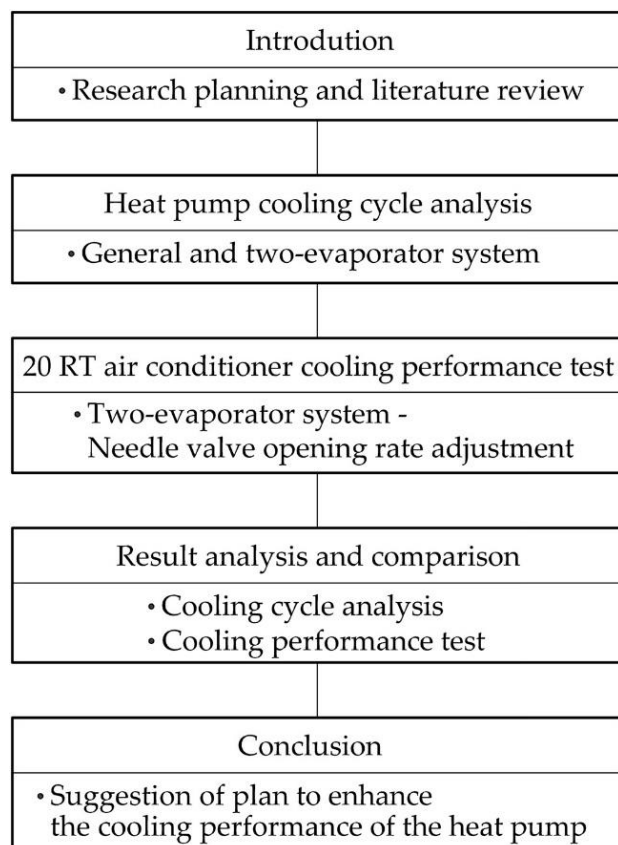


Figure 2. Research flow chart.

2.1. Heat Pump Cycle Analysis

Prior to the experiment, a cycle analysis was performed to evaluate the cooling performance based on predetermined conditions as listed in Table 1. The difference in the condensation and evaporation temperatures and superheat and subcooling degrees were determined with reference to existing experimental results. The compressor adiabatic efficiency was set with reference to the performance table of the Copeland compressor model ZP234KCE-TFD. The indoor and outdoor dry-bulb and wet-bulb temperatures were determined with reference to the standard cooling test KS B ISO 13253: Ducted air-conditioners and air-to-air heat pumps—Testing and rating for performance [33]. The bypass coefficient of air passing through the evaporator, defined in Equation (1), was calculated using experimental data. The number of thermodynamic states required for cycle analysis was calculated using the Engineering Equation Solver (EES) program.

$$B_{evap} = \frac{t_e - t_{evap.c}}{t_i - t_{evap.c}} \quad (1)$$

Table 1. Input conditions for cycle analysis.

Item		Value	Item		Value
Indoor	Dry-bulb temperature	27 °C	Evaporation temperature difference	20 °C	
	Wet-bulb temperature	19 °C	Condensation temperature difference	14 °C	
Outdoor	Dry-bulb temperature	35 °C	Superheat degree	5 °C	
	Wet-bulb temperature	24 °C	Subcooling degree	3 °C	
Compressor adiabatic efficiency		69.7%	Bypass coefficient	12%	

2.1.1. General Heat Pump System Configuration

A typical heat pump system consists of one compressor, one condenser, one expansion valve, and one evaporator, and the refrigerant circulation involves compression, condensation, expansion, and evaporation, in order. Figure 3 shows the configuration and pressure–enthalpy (P–h) diagram of a general heat pump system. Equations (2)–(4) can be used to calculate the cooling coefficient of performance (COP) of the system.

$$\dot{Q}_{evap} = \dot{m}(h_1 - h_4) \tag{2}$$

$$\dot{W}_{comp} = \dot{m}(h_2 - h_1) \tag{3}$$

$$COP_c = \frac{\dot{Q}_{evap}}{\dot{W}_{evap}} \tag{4}$$

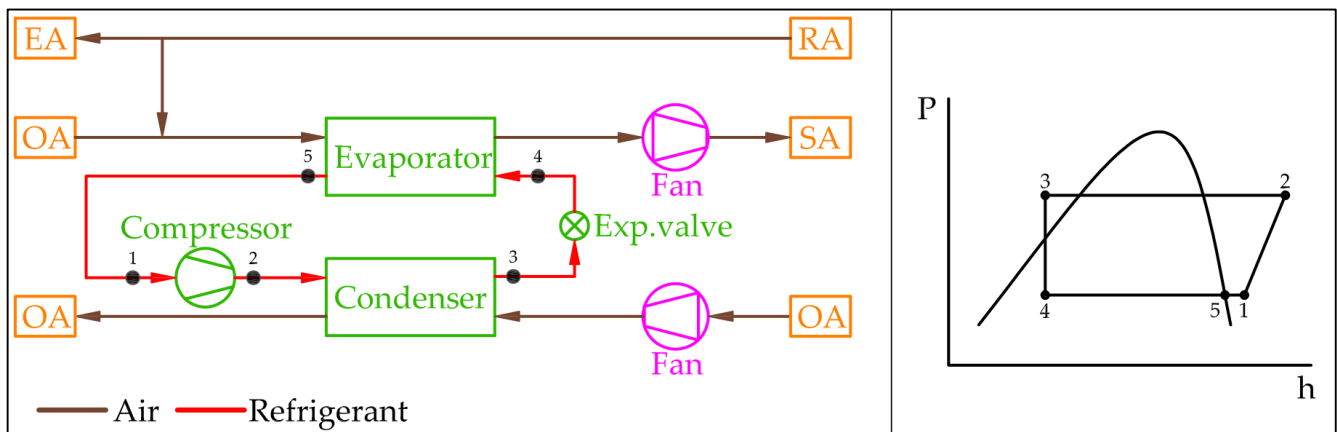


Figure 3. Configuration and P–h diagram of a general heat pump system.

2.1.2. Two-Evaporator Heat Pump System Configuration

The two-evaporator heat pump system consists of one compressor, one condenser, two expansion valves, and two evaporators. Like a general heat pump system, the refrigerant repeats the steps of compression, condensation, expansion, and evaporation in a cycle. The difference is that the refrigerant that has passed through the primary evaporator passes through a separate vapor–liquid separator and is separated into a vapor refrigerant and a liquid refrigerant. The separated vapor refrigerant is sent to the compressor and the liquid refrigerant is sent to the secondary evaporator. Figure 4 is a two-evaporator system configuration and P–h diagram [34]. In Figure 4, state a is the exit of 1st stage compression and state b is a mixture of state 6 and state a. Equations (5)–(11) were used to calculate the cooling COP of the two-evaporator heat pump system.

$$\dot{Q}_{evap1} = \dot{m}(1 - f)(h_1 - h_8) \tag{5}$$

$$\dot{Q}_{evap2} = \dot{m}(h_5 - h_4) \tag{6}$$

$$\dot{Q}_{t.evap} = \dot{Q}_{evap1} + \dot{Q}_{evap2} \tag{7}$$

$$\dot{W}_{comp1} = \dot{m}(1 - f)(h_a - h_1) \tag{8}$$

$$\dot{W}_{comp2} = \dot{m}(h_2 - h_b) \tag{9}$$

$$\dot{W}_{t.comp} = \dot{W}_{comp1} + \dot{W}_{comp2} \tag{10}$$

$$COP_c = \frac{\dot{Q}_{t.evap}}{\dot{W}_{t.comp}} \tag{11}$$

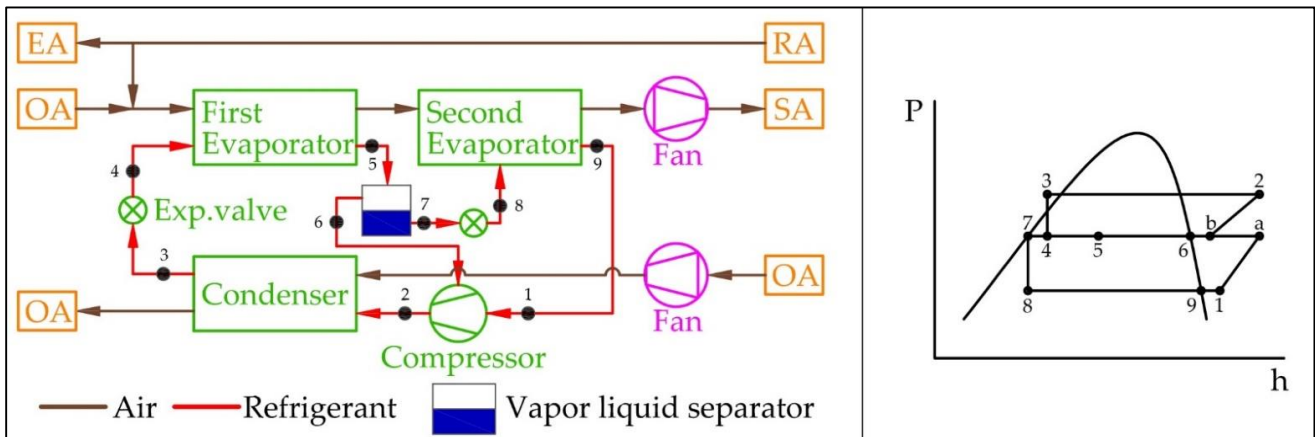


Figure 4. Two-evaporator heat pump system and P-h diagram.

2.1.3. Cycle Analysis Result

Table 2 summarizes the results of analyzing the cycles of general and two-evaporator heat pump systems using the EES program. The general heat pump system exhibits a compression work, evaporation capacity, and cooling COP of 44.5 kW, 151.7 kW, and 3.41, respectively. The compression work, evaporative heat, and cooling COP of the two-evaporator heat pump systems are 43.4 kW, 159.3 kW, and 3.68, respectively. The cooling COP of the two-evaporator heat pump system is approximately 0.27 (7.92%) higher than that of the general heat pump system, and thus, the heat pump performance was expected to be enhanced in the experiment.

Table 2. Results of the cycle analysis of general and two-evaporator heat pump systems.

Item	Symbol	Value	
		General	Two-Evaporator
Compression work	\dot{W}_{comp}	44.5 kW	43.4 kW
Evaporation capacity	\dot{Q}_{evap}	151.7 kW	159.3 kW
Cooling COP	COP_c	3.41	3.68

2.2. Air Conditioner Experiment

2.2.1. 20 RT (70 kW) Air Conditioner Specification

Table 3 lists the specifications of the air conditioner for the 20 RT (70 kW) two-evaporator heat pump system, and Figure 5 shows images of the air-conditioning system. The cooling capacity, refrigerant, compressor capacity, blower air volume flow rate, and blower static pressure of the air conditioner are 65.1 kW, R410A, 15 kW, 150 m³/min, and 20 mmAq, respectively. The cooling capacity of the primary evaporator is about 37 kW (32,000 kcal/h), and the cooling capacity of the secondary evaporator is about 34 kW (29,000 kcal/h). According to GSEED (Green Standard for Energy and Environmental Design of Buildings, www.gseed.or.kr (accessed on 1 May 2020) of Korea, R410A is classified

as an eco-friendly refrigerant [35]. In GSEED certification, for refrigerant, if ODP is less than 0.003 and GWP is less than 3000, then it is considered an eco-friendly refrigerant. For R410A, ODP is 0 and GWP is 1730, thus qualifies the criteria of eco-friendly refrigerant in GSEED. Though GWP of R410A is low but not zero, this refrigerant cannot be a permanent solution and must be replaced with alternative, of which both ODP and GWP are zero or infinitesimally small. R410A is a mixture of R32 and R125 and is a zeotropic, meaning temperature changes during constant pressure condensation and evaporation. Condenser and evaporator designs are affected by this temperature glide during phase change. Currently, research on refrigerants with a lower GWP than R410A is carried out actively worldwide. As a result of comparing performance of various refrigerants with experiment, Guilherme and Pico [36] confirmed that COP could be increased by 1.5% and 1.3%, respectively, when DR55 (R452b) and DR5A (R456b) were applied to equipment designed with R410A. In particular, DR5A (R456b) can be expected to increase COP by about 5.5–7.1% due to low compressor energy consumption, so it is said that it is appropriate to use it as an alternative refrigerant. Therefore, when an alternative refrigerant that can replace R410A is applied to two-evaporator system, it is expected that it will not significantly deviate from the results of this study.

Table 3. Specifications of the 20 RT (70 kW) air conditioner.

Item	Value	Item	Value
Compressor	Scroll type	Cooling capacity	65.1 kW
Compressor capacity	15 kW	Heating capacity	76.7 kW
Blower volumetric flow	150 CMM	Evaporator coil	3/8", 4R × 48S × 800EL
Blower static pressure	20 mmAq	Accumulator	20 HP

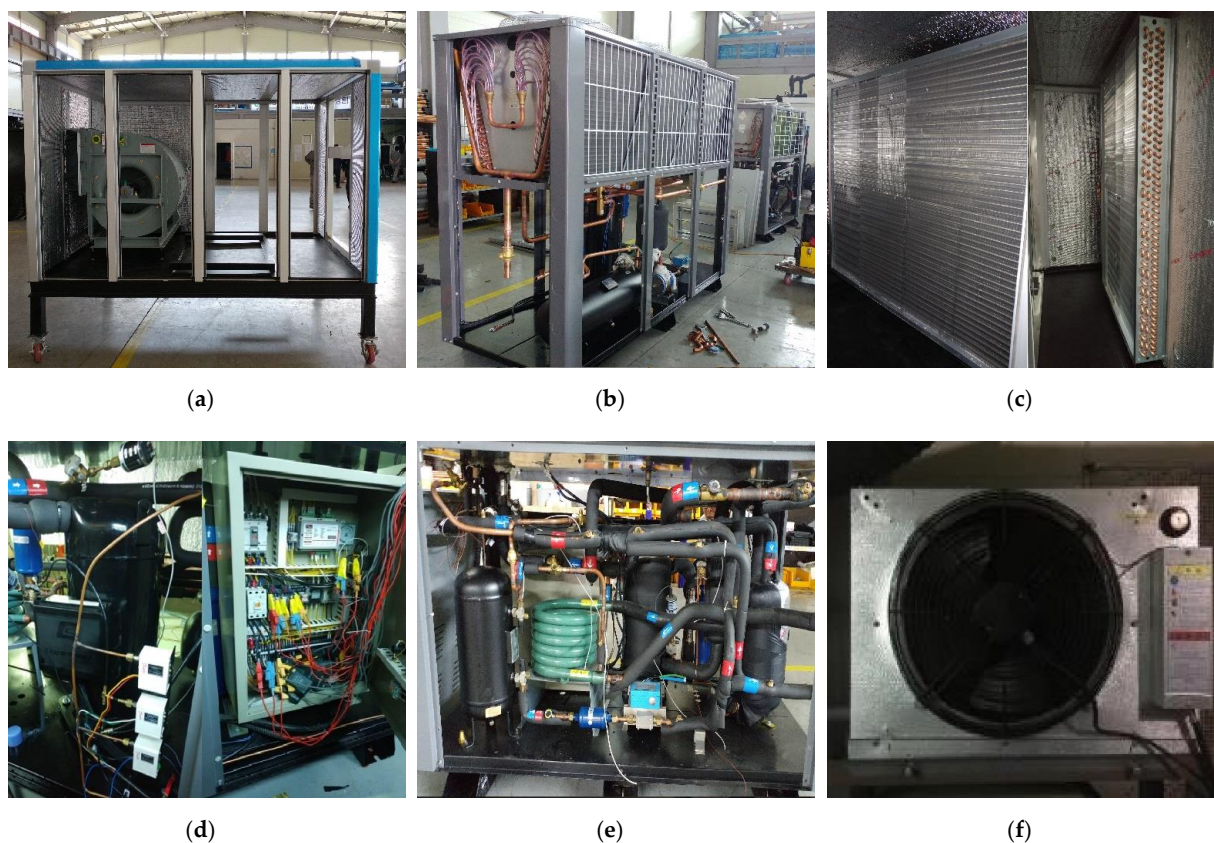


Figure 5. (a) Air conditioner frame, supply fan; (b) Outdoor condensing coil; (c) Air conditioner coil; (d) Compressor, control panel; (e) Air conditioner unit piping connection; (f) Cooler for the outdoor unit.

2.2.2. System Diagram and Data Measurement Location

Figure 6 schematically illustrates the configuration of the 20 RT (70 kW) two-evaporator heat pump system and data measurement locations. To increase the accuracy of the experimental results, both the air-side and refrigerant-side data were acquired. Table 4 shows the types of data obtained at the measurement locations.

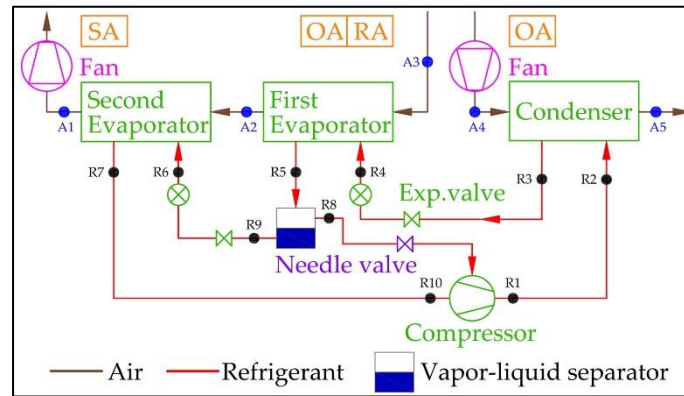


Figure 6. System diagram and data measurement locations for the 20 RT (70 kW) air conditioner system.

Table 4. Measurement location and item.

Location	Item	Location	Item	Location	Item
A1	T, H, \dot{V}	R1	T, P	R6	T, P
A2	T, H	R2	T, P	R7	T, P
A3	T, H	R3	T, P, \dot{m}	R8	T, P
A4	T, H	R4	T, P	R9	T, P, \dot{m}
A5	T, H	R5	T, P	R10	T, P
Compressor	E	Supply fan	E	Condenser fan	E

2.2.3. Measuring Equipment and Specifications

Tables 5–10 summarize the equipment used to measure the experimental data and the corresponding specifications. All equipment used in the experiment was used after calibration within the error range.

Table 5. Airflow sensor specification.

	Model	Kanomax TAB master 6710		
	Measurement Specifications	Airflow	Range Accuracy	40 to 4250 m ³ /h ±3% of reading ±8 m ³ /h
		Temperature	Range Accuracy	0 to 50 °C ±0.5 °C
		Humidity	Range Accuracy	0 to 100% RH ±3% RH

Table 6. Data logger specification.

	Model	Graphtec MIDI logger GL840		
	Measurement Specifications	Voltage	Range Accuracy	20 mV to 100 V ±0.05%
		Temperature	Thermocouple Accuracy	R, S, B, K, E, T, J, N, W ±1.1 °C

Table 7. Mass flow meter specification.

	Model	Rheonik RHM 08	
	Measurement Specifications	Typical application range Max. pressure Temperature Accuracy	0.3 up to 50 kg/min 1254 bar/18,057 psi −196 up to 400 °C 0.1%

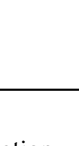
Table 8. Power meter specification.

	Model	Yokogawa CW240	
	Measurement Specifications	Voltage range Current mode Wiring mode Time interval	0/150, 0/300, 0/600, 0/1000 V 2/50/200/500/1000 A 1P2W/1P3W/1P3W/3P3W/3P4W 0.1/0.2/0.5 Each waveform

Table 9. Temperature and humidity sensor specification.

	Model	SRN-300
	Temperature range Humidity range	0 to 70 °C (±0.3 °C) 0 to 100% (±3% RH)

Table 10. Pressure sensor specification.

	Model	SETRA 206
	Pressure range Operation temperature	0 to 500 psi (±0.13%) −40 to 85 °C

2.2.4. Air Conditioning Room Simulator

Figure 7 schematically illustrates the simulator for the 20 RT (70 kW) air conditioner cooling performance test. The air input to the air conditioner is a mixture of indoor and outdoor air, supplied to the room after passing through evaporators 1 and 2. In the space in which the condenser is installed, the temperature may continuously increase owing to the heat emitted by the condenser. Therefore, a separate cooler is installed to maintain a constant temperature. Figure 8 shows the components in the air-conditioning room and simulator used in the experiment.

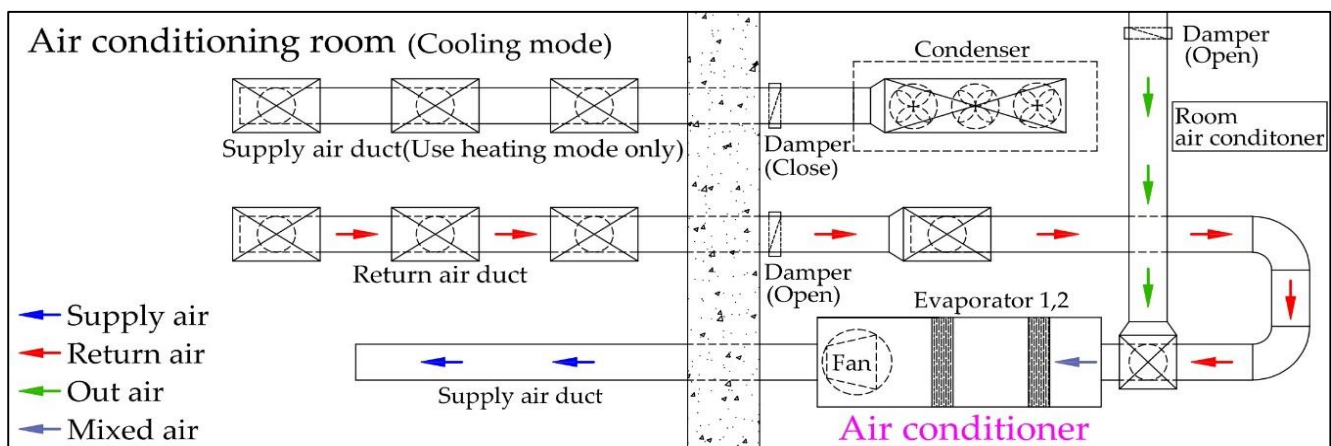


Figure 7. Air conditioning simulator layout.

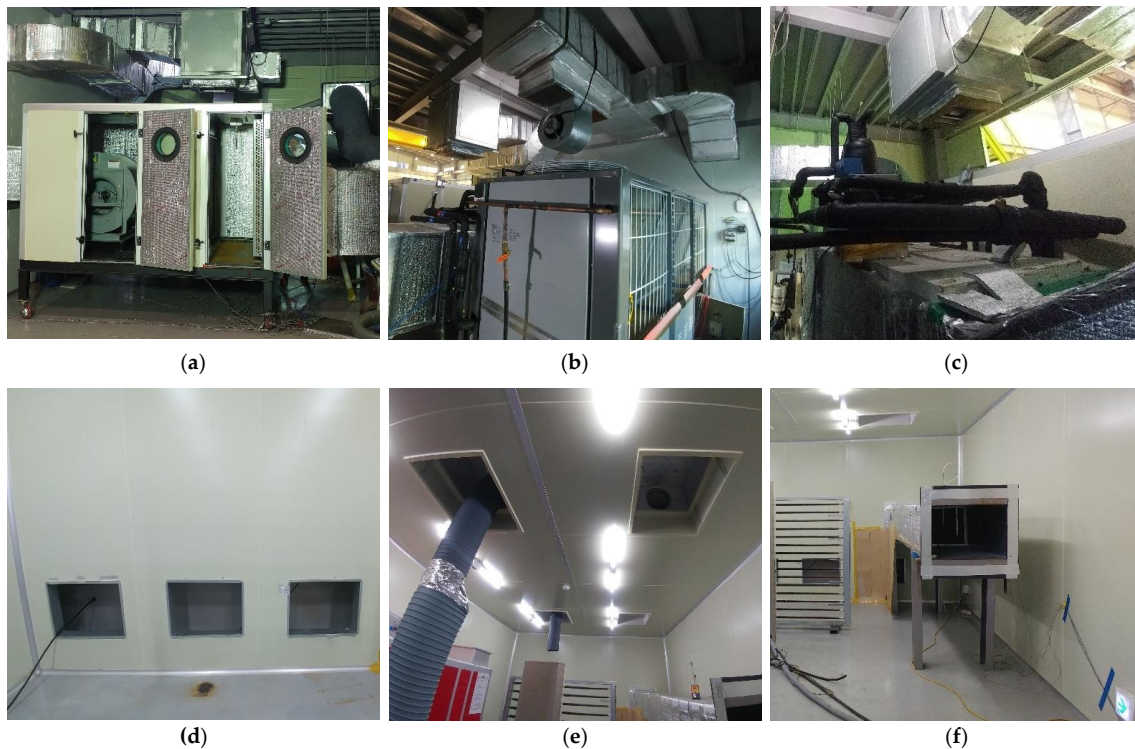


Figure 8. (a) Air conditioner; (b) Ceiling duct of the outdoor unit; (c) Refrigerant pipe of the vapor–liquid separator; (d) Indoor return chamber inlet; (e) Indoor air supply and exhaust duct; (f) Indoor air supply duct.

2.2.5. Test Condition and Method

The test was conducted with reference to the standard cooling test described in KS B ISO 13253 [33]. According to the standard cooling test conditions, the indoor and outdoor inflow dry-bulb temperatures (wet-bulb temperatures) were set as 27 °C (19 °C), and 35 °C (24 °C), respectively. Table 11 specifies the cooling capacity evaluation conditions based on the standard climate of the standard cooling test conditions.

Table 11. Cooling test conditions in standard climate.

Item	Dry-Bulb Temperature	Wet-Bulb Temperature
Indoor inflow air temperature	27 °C	19 °C
Outdoor inflow air temperature	35 °C	24 °C

In the experiment, the refrigerant that passed through the primary evaporator was separated into vapor and liquid forms by a vapor–liquid separator and input to the compressor and secondary evaporator, respectively. The amount of vapor refrigerant was adjusted using a needle valve to examine the influence of this parameter on the cooling performance. The needle valve opening was adjusted to 0%, 50%, and 100%. Table 12 describes the configuration of the two-evaporator cooling performance test. Data measurement was initiated as soon as the air conditioner started operating. To obtain steady-state data, the air conditioner was operated for more than 30 min.

Table 12. Two-evaporator test method.

Experiment Method	
No 1.	Needle valve opening 0% (No vapor refrigerant is sent to the compressor)
No 2.	Needle valve opening 50%
No.3	Needle valve opening 100%

3. Results and Discussions

The following sections describe the experimental results obtained for different needle valve opening (0%, 50%, 100%). To ensure repeatability, the experiment for each configuration was repeated five times. The measured data were divided into air side and refrigerant side, and the data associated with a stable state were primarily used. The data measurement locations specified in the tables of experimental results correspond to those shown in Figure 6. Moreover, A represents air, H is the humidity, M_F is the mass flow rate, P is the pressure, R represents the refrigerant, T is the temperature, V_F is the volumetric flow rate, and W_P is the compressor power. The cooling COP was calculated according to the experimental results as the heat of evaporation associated with the compressor power.

3.1. Valve Opening 0%

Table 13 presents the results of five experiments on the air side. When the primary evaporator inlet (A3) and outlet (A2) temperatures are 26.8–27.3 °C and 15.0–15.5 °C, the humidity values are 51.9–52.5% and 99.2–99.3%, respectively. When the secondary evaporator outlet (A1) temperature is 13.5–13.9 °C, the humidity is 98.7–98.8%. The volumetric flow rates range from 9510 to 9545 m³/h, with an average of approximately 9531 m³/h.

Table 13. Air side measurement result (five times).

No	A1		A2		A3		V_F (m ³ /h)
	T (°C)	H (%)	T (°C)	H (%)	T (°C)	H (%)	
1	13.7	98.8	15.2	99.2	27.0	52.3	9542
2	13.8	98.7	15.5	99.3	27.3	51.9	9545
3	13.5	98.7	15.5	99.2	26.9	52.5	9510
4	13.9	98.8	15.0	99.2	27.1	52.1	9511
5	13.8	98.7	15.3	99.3	26.8	52.3	9545

Table 14 shows the results of five experiments on the refrigerant side. When the primary evaporator inlet (R4) and outlet (R5) refrigerant temperatures are 15.6–15.9 °C and 21.2–23.5 °C, the pressure values are 1279–1290 kPa and 1269–1296 kPa, respectively. When the secondary evaporator inlet (R6) and outlet (R7) refrigerant temperatures are 14.1–14.7 °C and 21.2–24.3 °C, the pressure values are 1202–1216 kPa and 969–981 kPa, respectively.

Table 14. Refrigerant side measurement result (five times).

No	R4		R5		R6		R7		M_F (kg/s)	W_P (kW)
	T (°C)	P (kPa)								
1	15.7	1283	22.4	1289	14.7	1210	23.4	971	0.3668	18.5
2	15.9	1289	23.4	1294	14.5	1203	24.3	976	0.3713	18.6
3	15.7	1281	23.5	1296	14.5	1202	23.4	981	0.3675	18.7
4	15.6	1279	21.5	1278	14.2	1209	22.9	973	0.3668	18.7
5	15.9	1290	21.2	1269	14.1	1216	21.2	969	0.3752	18.6

Table 15 specifies the heat of evaporation on the air side and refrigerant side and the cooling COP calculated from the experimental results. The heat of evaporation on the air and refrigerant sides is 60.4–62.3 kW and 63.4–64.2 kW, with average values of 61.3 kW, and 63.8 kW, respectively. The cooling COP on the air and refrigerant sides is 3.03–3.23 and 3.26–3.34, with average values of 3.14 and 3.31, respectively. The average cooling COP on the refrigerant side is 0.17 lower than that on the air side, indicating that the average heat loss on the air side is approximately 5.1%.

Table 15. Air side and refrigerant side cooling performance result (five times).

No	Cooling Capacity (kW)		Cooling Coefficient of Performance	
	Air	Refrigerant	Air	Refrigerant
1	61.0	63.8	3.19	3.30
2	61.6	64.0	3.21	3.32
3	62.3	64.2	3.23	3.34
4	60.4	63.5	3.06	3.32
5	61.1	63.4	3.03	3.26
Average	61.3	63.8	3.14	3.31

3.2. Valve Opening 50%

Table 16 presents the results of five experiments on the air side. When the primary evaporator inlet (A3) and outlet (A2) temperatures are 27.0–27.3 °C and 15.1–15.7 °C, the humidity values are 51.0–52.8% and 99.1–99.3%, respectively. When the secondary evaporator outlet (A1) temperature is 13.3–13.8 °C, the humidity is 98.8–99.2%. The volumetric flow rates range from 9755 to 9771 m³/h, with an average of approximately 9761 m³/h.

Table 16. Air side measurement result (five times).

No	A1		A2		A3		V _F (m ³ /h)
	T (°C)	H (%)	T (°C)	H (%)	T (°C)	H (%)	
1	13.3	98.9	15.1	99.3	27.2	51.0	9755
2	13.5	99.2	15.7	99.1	27.0	52.2	9758
3	13.5	98.8	15.2	99.3	27.1	51.7	9765
4	13.8	98.8	15.5	99.2	27.3	52.8	9771
5	13.4	98.8	15.7	99.1	27.2	51.0	9755

Table 17 shows the results of five experiments on the refrigerant side. When the primary evaporator inlet (R4) and outlet (R5) refrigerant temperatures are 15.3–15.8 °C and 21.2–22.6 °C, the pressure values are 1269–1281 kPa and 1273–1286 kPa, respectively. When the secondary evaporator inlet (R6) and outlet (R7) refrigerant temperatures are 12.2–13.2 °C and 23.3–25.5 °C, the pressure values are 1158–1190 kPa and 965–987 kPa, respectively.

Table 17. Refrigerant side measurement result (five times).

No	R4		R5		R6		R7		M _F (kg/s)	W _P (kW)
	T (°C)	P (kPa)								
1	15.6	1278	21.2	1273	13.2	1190	23.3	987	0.3824	18.9
2	15.8	1281	22.4	1282	12.8	1178	25.4	981	0.3861	18.9
3	15.3	1269	21.6	1275	12.2	1158	24.4	976	0.3849	18.7
4	15.5	1274	22.6	1286	12.8	1177	23.5	983	0.3766	18.9
5	15.4	1271	21.4	1274	12.8	1179	25.5	965	0.3812	18.9

Table 18 specifies the heat of evaporation of the air side and refrigerant side and the cooling COP calculated from the experimental results. The heat of evaporation on the air and refrigerant sides is 63.5–64.9 kW and 64.9–66.3 kW, with average values of 64.2 kW and 65.8 kW, respectively. The cooling COP on the air and refrigerant sides is 3.36–3.43 and 3.42–3.54, with average values of 3.40 and 3.49, respectively. The average cooling COP on the refrigerant side is 0.09 lower than that on the air side, indicating that the average heat loss on the air side is approximately 2.6%.

Table 18. Air side and refrigerant side cooling performance result (five times).

No	Cooling Capacity (kW)		Cooling Coefficient of Performance	
	Air	Refrigerant	Air	Refrigerant
1	64.8	66.3	3.43	3.51
2	63.9	66.3	3.38	3.51
3	63.8	66.2	3.41	3.54
4	64.9	64.9	3.43	3.42
5	63.5	65.5	3.36	3.47
Average	64.2	65.8	3.40	3.49

Uncertainty propagation analysis has been carried out for air-side cooling capacity to determine the uncertainty of the results in Table 18. Air-side cooling capacity can be calculated with Equation (12).

$$\dot{Q}_{evap,a} = \rho C_{pa} \dot{V} \Delta T \quad (12)$$

where, $\dot{Q}_{evap,a}$ is air-side cooling capacity, ρ is air density, C_{pa} is constant pressure specific heat of air, \dot{V} is volumetric air flow rate, and ΔT is temperature difference between inlet and outlet air passing through the evaporator.

Uncertainty of air-side cooling capacity is expressed in Equation (13) [37].

$$\left(w_{\dot{Q}_{evap,air}} \right)^2 = \left(w_{\dot{V}} \frac{\partial \dot{Q}_{evap,a}}{\partial \dot{V}} \right)^2 + \left(w_{\Delta T} \frac{\partial \dot{Q}_{evap,a}}{\partial \Delta T} \right)^2 \quad (13)$$

where w is uncertainty. Uncertainty of volumetric air flow rate $w_{\dot{V}}$ is 8 m³/h as given in Table 5, and uncertainty of temperature w_T is 0.2 °C. From Table 16, the nominal value of $\dot{Q}_{evap,a}$ is 64 kW, the air flow rate \dot{V} is 9531 m³/h, and the temperature difference ΔT is 12.5 °C. For air, density ρ is assumed as 1.2 kg/m³, and constant specific heat 1.004 kJ/kg °C. Using Equation (12) for deriving partial derivatives in Equation (13), the uncertainty of air-side cooling capacity $\dot{Q}_{evap,a}$ becomes 0.64 kW or 1.0%.

3.3. Valve Opening 100%

Table 19 presents the results of five experiments on the air side. When the primary evaporator inlet (A3) and outlet (A2) temperatures are 27.0–27.2 °C and 14.7–15.2 °C, the humidity values are 50.2–51.5% and 99.3–99.5%, respectively. When the secondary evaporator outlet (A1) temperature is 12.8–13.0 °C, the humidity is 99.1–99.3%. The volumetric flow rates range from 9764 to 9787 m³/h, with an average of approximately 9773 m³/h.

Table 19. Air side measurement result (five times).

No	A1		A2		A3		V _F (m ³ /h)
	T (°C)	H (%)	T (°C)	H (%)	T (°C)	H (%)	
1	12.9	99.3	14.9	99.3	27.1	51.1	9772
2	13.0	99.2	15.1	99.5	27.2	50.9	9764
3	12.8	99.3	14.8	99.5	27.0	51.2	9787
4	12.8	99.3	14.7	99.4	27.2	50.2	9764
5	13.0	99.3	15.2	99.3	27.0	51.5	9780

Table 20 shows the results of five experiments on the refrigerant side. When the primary evaporator inlet (R4) and outlet (R5) refrigerant temperatures are 14.8–15.1 °C and 22.9–23.6 °C, respectively, the pressure values are 1248–1261 kPa and 1287–1299 kPa,

respectively. When the secondary evaporator inlet (R6) and outlet (R7) refrigerant temperatures are 12.2–12.8 °C and 24.2–25.5 °C, the pressure values are 1158–1179 kPa and 946–981 kPa, respectively.

Table 20. Refrigerant side measurement result (five times).

No	R4		R5		R6		R7		M _F (kg/s)	W _P (kW)
	T (°C)	P (kPa)								
1	15.1	1259	23.6	1299	12.3	1162	25.5	978	0.3838	18.1
2	14.9	1254	22.9	1287	12.8	1177	24.2	969	0.3889	18.3
3	15.1	1261	23.1	1295	12.2	1158	24.3	946	0.3892	18.5
4	14.8	1248	23.1	1296	12.8	1178	24.2	981	0.3889	18.3
5	15.0	1256	23.0	1288	12.8	1179	24.9	948	0.3845	18.1

Table 21 specifies the heat of evaporation of the air side and refrigerant side and the cooling COP calculated from the experimental results. The heat of evaporation on the air and refrigerant sides is 66.6–67.9 kW and 68.1–68.9 kW, respectively, with average values of 67.1 kW and 68.5 kW, respectively. The cooling COP on the air and refrigerant sides is 3.61–3.73 and 3.72–3.78 on the air side, with average values of 3.68 and 3.76, respectively. The average cooling COP on the refrigerant side is 0.08 lower than that on the air side, indicating that the average heat loss on the air side is approximately 2.1%.

Table 21. Air side and refrigerant side cooling performance result (five times).

No	Cooling Capacity (kW)		Cooling Coefficient of Performance	
	Air	Refrigerant	Air	Refrigerant
1	67.4	68.3	3.73	3.78
2	67.9	68.7	3.71	3.75
3	66.8	68.9	3.61	3.72
4	66.8	68.6	3.66	3.76
5	66.6	68.1	3.69	3.77
Average	67.1	68.5	3.68	3.76

3.4. Main Findings and Remarks

Figure 9 shows the average cooling COP calculated from the experimental results of the air and refrigerant sides for different valve openings. The average cooling COP for the air and refrigerant sides differs by approximately 5.1%, 2.6%, and 2.1% when the valve opening is 0%, 50%, and 100%, respectively. In all the experiments, the cooling COP for the refrigerant side is higher than that of the air side, attributable to the heat loss that occurs when cooling heat from the refrigerant side is transferred to the air side. Because the error is within 5%, the results are not significantly different. Therefore, the experimental results were comparatively analyzed based on the air-side data.

Table 22 lists the average (of five air side experiments) temperature, total evaporative heat, and cooling COP for different measurement locations and valve openings. A represents air, COP is the cooling COP, and T_H is the total heat evaporation. The numbers represent the measurement positions in Figure 6.

In the experiments, the average temperature of the inlet (A3) of the primary evaporator is 27.02–27.16 °C, which satisfies the standard cooling test condition of 27 °C. For all valve openings, the average air temperature difference between the inlet (A3) and outlet (A2) of the primary evaporator is almost constant (11.72–12.16 °C). The average air temperatures at the inlet (A2) and outlet (A1) of the secondary evaporator differ by 1.56 °C, 1.94 °C, and 2.04 °C at valve openings of 0%, 50%, and 100%, respectively. The average total evaporative heat and cooling COP are 61.30 kW and 3.14, respectively, when the valve opening is 0%, 64.20 kW and 3.40 when the valve opening is 50%, and 67.10 kW and 3.68 when the valve

opening is 100%. A higher valve opening corresponds to a higher evaporator cooling effect, and thus, a higher cooling COP.

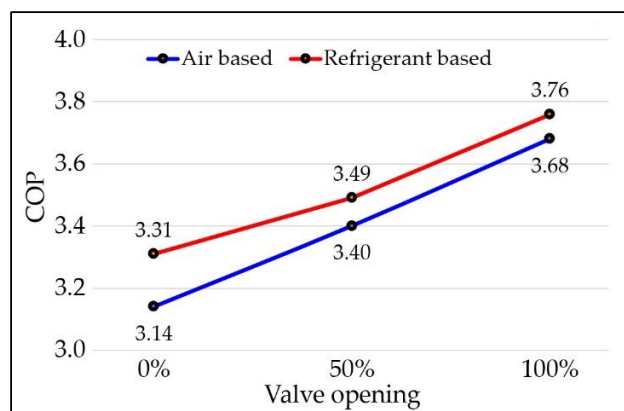


Figure 9. Average COP results for the air and refrigerant sides for different valve openings.

Table 22. Average data of five experiments based on the air side.

Division	A1 (°C)	A2 (°C)	A3 (°C)	T _H (kW)	COP
Valve opening (0%)	13.74	15.30	27.02	61.30	3.14
Valve opening (50%)	13.50	15.44	27.16	64.20	3.40
Valve opening (100%)	12.90	14.94	27.10	67.10	3.68

4. Conclusions and Future Work

To enhance the cooling performance of a heat pump, a 20 RT (70 kW) two-evaporator heat pump air conditioner was manufactured and tested. The refrigerant passing through the primary evaporator was separated into a vapor and liquid using a vapor–liquid separator, and the vapor refrigerant was input into a compressor. The influence of the amount of vapor refrigerant on the cooling performance of the heat pump was analyzed. The amount of vapor refrigerant was controlled by setting the needle valve opening as 0%, 50%, and 100%. Experiments for each case were repeated five times, and data on the air and refrigerant sides were measured and compared. The results could be summarized as follows.

- (1) According to the heat pump cycle analysis, the COP values of the general system and two-evaporator system were 3.41 and 3.68, respectively, indicating that the cooling performance of the two-evaporator system was approximately 7.92% higher.
- (2) According to the cooling performance test, heat loss occurred regardless of the change in valve opening, so the air-side COP was about 2–5% lower than the refrigerant-side COP.
- (3) When the valve opening was 0%, the average cooling capacity based on the air side was 61.30 kW and the average COP was 3.14.
- (4) When the valve opening was 50%, the average cooling capacity based on the air side was 64.20 kW and the average COP was 3.40.
- (5) When the valve opening was 100%, the average cooling capacity based on the air side was 67.10 kW and the average COP was 3.68.
- (6) When the valve opening was 100%, the average cooling capacity and COP were 5.8 kW (9.46%) and 0.54 (17.20%) higher than those when the valve opening was 0%.
- (7) The COP of the double evaporator heat pump system was 3.68 in the cycle analysis and 3.76 in the refrigerant side experiment with 100% valve opening degree, which was almost similar. Therefore, it was judged that the double evaporator heat pump system had better cooling performance than the general heat pump system in the experiment as in the result of item (1).

The findings demonstrated that the cooling effect in the secondary evaporator was enhanced when a larger amount of vapor refrigerant, derived from the refrigerant passing

through the primary evaporator, was input to the compressor, and the cooling performance of the heat pump was effectively enhanced. The proposed technology is thus an effective platform to enhance the heat pump cooling performance.

Future research can be aimed at performing economic analyses and comparisons for general and two-evaporator heat pump systems. In particular, we want to study the energy-saving effect according to the cooling load when applied to home, corporate, and industrial air conditioners and find improvements. Since industrial air conditioners require a large amount of energy, it is expected that the ripple effect will be large as the energy-saving effect for each facility is large and the economic feasibility is good compared to the investment. Furthermore, since these industrial air conditioners are used in various environments, we want to conduct experiments in high- and low-temperature climates. Through this study, it is hoped that the double evaporator heat pump system will be applied in various fields to help save energy.

Author Contributions: Conceptualization, W.-S.Y.; methodology, W.-S.Y.; experiment, W.-S.Y.; software, W.-S.Y.; validation, Y.I.K.; formal analysis, W.-S.Y.; investigation, W.-S.Y.; resources, W.-S.Y.; data curation W.-S.Y.; writing—original draft preparation, W.-S.Y.; writing—review and editing, Y.I.K.; visualization, W.-S.Y.; supervision, Y.I.K.; project administration, Y.I.K.; funding acquisition, Y.I.K. All authors have read and agreed to the published version of the manuscript.

Funding: This study was supported by the Research Program funded by the SeoulTech (Seoul National University of Science and Technology).

Institutional Review Board Statement: Not applicable.

Informed Consent Statement: Not applicable.

Conflicts of Interest: The authors declare no conflict of interest.

Nomenclature

A	air
B	bypass factor
C	specific heat (kJ/kg °C)
COP	coefficient of performance
E	electric power
f	bypass coefficient of refrigerant
H	humidity
h	enthalpy (kJ/kg)
\dot{m}	mass flow rate (kg/s)
P	pressure
\dot{Q}	heat capacity (kW)
R	refrigerant
$T(t)$	temperature (°C)
\dot{V}	volumetric air flow rate (m ³ /h)
\dot{W}	work (kW)
w	uncertainty
ρ	air density (kg/m ³)
Δ	difference

Subscript

a	air
c	cooling
$evap.c$	evaporator coil
$comp$	compressor
e	exit
$evap$	evaporator
i	inlet
p	constant pressure
t	total

References

1. Mun, E.J. Thermal Comfort Analysis on a Space and Seasonal Performance Evaluation of a Building with Multi-type Air Source Heat Pump System. Master's Thesis, Seoul National University, Seoul, Korea, 2015.
2. Yang, L.; Yan, H.; Lam, J.C. Thermal comfort and building energy consumption implications—A review. *Appl. Energy* **2014**, *115*, 164–173. [[CrossRef](#)]
3. Song, M.; Mao, N.; Xu, Y.; Deng, S. Challenges in, and the development of, building energy saving techniques, illustrated with the example of an air source heat pump. *Therm. Sci. Eng. Prog.* **2019**, *10*, 337–356. [[CrossRef](#)]
4. Von Cube, H.L.; Steimle, F. *Heat Pump Technology*; Elsevier: Amsterdam, The Netherlands, 2013.
5. Chua, K.J.; Chou, S.K.; Yang, W.M. Advances in heat pump systems: A review. *Appl. Energy* **2010**, *87*, 3611–3624. [[CrossRef](#)]
6. Lee, M.J.; Lee, D.K.; Park, C.; Park, J.H.; Jung, T.Y.; Kim, S.K.; Hong, S.C. Prediction of Heating and Cooling Energy Consumption in Residential Sector Considering Climate Change and Socio-Economic. *Environ. Impact Assess.* **2015**, *24*, 487–498. [[CrossRef](#)]
7. Seo, J.H.; Bang, Y.M.; Lee, M.Y. Investigation on the Performance of Special Purpose Automotive Air-Conditioning System Using Dual Refrigeration Cycle. *Trans. Korean Soc. Mech. Eng.-B* **2016**, *40*, 213–220. [[CrossRef](#)]
8. Wang, Q.; Li, T.; Jia, Y.; Zhang, W. Thermodynamic performance comparison of series and parallel two-stage evaporation vapor compression refrigeration cycle. *Energy Rep.* **2021**, *7*, 1616–1626. [[CrossRef](#)]
9. Yataganbaba, A.; Kilicarslan, A.; Kurtbas, I. Exergy analysis of R1234yf and R1234ze as R134a replacements in a two evaporator vapour compression refrigeration system. *Int. J. Refrig.* **2015**, *60*, 26–37. [[CrossRef](#)]
10. Hu, H.; Ji, J.; Xie, L.; Li, Y.; Zhang, X. Performance investigation of a multi-connected heating tower heat pump system. *Int. J. Refrig.* **2022**, *135*, 154–163. [[CrossRef](#)]
11. Bae, S.M.; Nam, Y.J. Economic and environmental analysis of ground source heat pump system according to operation methods. *Geothermics* **2022**, *101*, 102373. [[CrossRef](#)]
12. Hu, B.; Xu, S.; Wang, R.Z.; Liu, H.; Han, L.; Zhang, Z.; Li, H. Investigation on advanced heat pump systems with improved energy efficiency. *Energy Convers. Manag.* **2019**, *192*, 161–170. [[CrossRef](#)]
13. Wu, W.; You, T.; Wang, J.; Wang, B.; Shi, W.; Li, X. A novel internally hybrid absorption-compression heat pump for performance improvement. *Energy Convers. Manag.* **2018**, *168*, 237–251. [[CrossRef](#)]
14. Vering, C.; Wüllhorst, F.; Mehrfeld, P.; Müller, D. Towards an integrated design of heat pump systems: Application of process intensification using two-stage optimization. *Energy Convers. Manag.* **2021**, *250*, 114888. [[CrossRef](#)]
15. Joo, Y.J.; Kang, H.; Ahn, J.H.; Lee, M.Y.; Kim, Y.C. Performance characteristics of a simultaneous cooling and heating multi-heat pump at partial load conditions. *Int. J. Refrig.* **2011**, *34*, 893–901. [[CrossRef](#)]
16. Vering, C.; Tanrikulu, A.; Mehrfeld, P.; Müller, D. Simulation-based design optimization of heat pump systems considering building variations. *Energy Build.* **2021**, *251*, 111310. [[CrossRef](#)]
17. Krütfeldt, H.; Vering, C.; Mehrfeld, P.; Müller, D. MILP design optimization of heat pump systems in German residential buildings. *Energy Build.* **2021**, *249*, 111204. [[CrossRef](#)]
18. Safa, A.A.; Fung, A.S.; Kumar, R. Heating and cooling performance characterization of ground source heat pump system by testing and TRNSYS simulation. *Renew. Energy* **2015**, *83*, 565–575. [[CrossRef](#)]
19. Luo, J.; Rohn, J.; Bayer, M.; Priess, A.; Wilkmann, L.; Xiang, W. Heating and cooling performance analysis of a ground source heat pump system in Southern Germany. *Geothermics* **2015**, *53*, 57–66. [[CrossRef](#)]
20. Çakır, U.; Çomaklı, K.; Çomaklı, Ö.; Karlı, S. An experimental exergetic comparison of four different heat pump systems working at same conditions: As air to air, air to water, water to water and water to air. *Energy* **2013**, *58*, 210–219. [[CrossRef](#)]
21. Zeng, R.; Zhang, X.; Deng, Y.; Li, H.; Zhang, G. Optimization and performance comparison of combined cooling, heating and power/ground source heat pump/photovoltaic/solar thermal system under different load ratio for two operation strategies. *Energy Convers. Manag.* **2020**, *208*, 112579. [[CrossRef](#)]
22. Hakkaki-Fard, A.; Eslami-Nejad, P.; Aidoun, Z.; Ouzzane, M. A techno-economic comparison of a direct expansion ground-source and an air-source heat pump system in Canadian cold climates. *Energy* **2015**, *87*, 49–59. [[CrossRef](#)]
23. Kong, R.; Deethayat, T.; Asanakham, A.; Kiatsiroat, T. Performance and economic evaluation of a photovoltaic/thermal (PV/T)-cascade heat pump for combined cooling, heat and power in tropical climate area. *J. Energy Storage* **2020**, *30*, 101507. [[CrossRef](#)]
24. Zhou, K.; Mao, J.; Li, Y.; Zhang, H. Performance assessment and techno-economic optimization of ground source heat pump for residential heating and cooling: A case study of Nanjing, China. *Sustain. Energy Technol. Assess.* **2020**, *40*, 100782. [[CrossRef](#)]
25. Lee, H.J.; Ahn, Y.N.; Jung, C.S.; Wang, Y.H.; Kim, J.Y. Study on Two-zone separated evaporation system's theory & Improvement of Cooling Performance, Fuel Efficiency. *Int. J. Automot. Technol.* **2013**, *20*, 689–697.
26. Zhang, C.; Wu, J.; Gao, J.; Huang, X. Experimental study of a novel double-effect evaporation concentration system for high temperature heat pump. *Desalination* **2020**, *491*, 114495. [[CrossRef](#)]
27. Baik, Y.J.; Kim, M.S.; Chang, K.C.; Lee, Y.S.; Kim, H.J. Potential Performance Enhancement of Dual Heat Pump Systems through Series Operation. *Korean Soc. Mech. Eng. Trans. B* **2012**, *38*, 797–802. [[CrossRef](#)]
28. Elliott, M.S.; Rasmussen, B.P. A model-based predictive supervisory controller for multi-evaporator HVAC systems. In Proceedings of the 2009 American Control Conference, St. Louis, MO, USA, 10–12 June 2009; pp. 3669–3674.
29. Mei, J.; Xia, X. Distributed control for a multi-evaporator air conditioning system. *Control. Eng. Pract.* **2019**, *90*, 85–100. [[CrossRef](#)]

30. Chen, W.H.; Mo, H.E.; Teng, T.P. Performance improvement of a split air conditioner by using an energy saving device. *Energy Build.* **2019**, *174*, 380–387. [[CrossRef](#)]
31. Chaiyat, N. Energy and economic analysis of a building air-conditioner with a phase change material (PCM). *Energy Convers. Manag.* **2015**, *94*, 150–158. [[CrossRef](#)]
32. Xu, H.; Tang, R.; Sun, J.; Xi, H. Experimental Study of Flow in the Gap of Needle Valve. In Proceedings of the JFPS International Symposium on Fluid Power, Dresden, Germany, 1–2 April 1999; Volume 4, pp. 437–442.
33. KS B ISO13253; Standard Cooling Test Conditions (Ducted Air-Conditioners and Air-to-Air Heat Pumps-Testing and Rating for Performance). Korean Agency for Technology and Standards: Eumseong-gun, Korea, 2018; pp. 10–12.
34. Wang, X.; Yu, J.; Xing, M. Performance analysis of a new ejector enhanced vapor injection heat pump cycle. *Energy Convers. Manag.* **2015**, *100*, 242–248. [[CrossRef](#)]
35. *Green Standard for Energy and Environmental Design*; G-SEED Detailed Criteria for Certification Examination; The Association for Computer-Aided Architectural Design Research in Asia (CAADRRIA): Nanjing, China, 2021; p. 44.
36. Guilherme, Í.F.; Pico, D.F.M.; dos Santos, D.D.O.; Bandarra Filho, E.P. A review on the performance and environmental assessment of R-410A alternative refrigerants. *J. Build. Eng.* **2022**, *47*, 103847. [[CrossRef](#)]
37. Wheeler, A.J.; Ganji, A.R. *Introduction to Engineering Experimentation*, 2nd ed.; Pearson Prentice Hall: Hoboken, NJ, USA, 2004.